

High RF power tests of the first 1.3 GHz fundamental power coupler prototypes for the SHINE project

Authors: Ma, Zhen-Yu, Zhao, Shen-Jie, Liu, Xu-Ming, Yu, Yue-Chao, Jiang, Hong-Ru, Zheng, Xiang, Chang, Qiang, Zhang, Zi-Gang, Xu, Kai, Wang, Yan, Zhao, Yu-Bin, Hou, Hong-Tao, Ma, Zhen-Yu, Hou, Hong-Tao

Date: 2021-12-31T10:32:27+00:00

Abstract

The Shanghai High Repetition Rate XFEL and Extreme Light Facility (SHINE) project will use 600 1.3 GHz fundamental power couplers, which are modified based on TTF-III power couplers, for continuous wave operation with input power up to approximately 7 kW. The first batch of 20 sets of 1.3 GHz coupler prototypes were fabricated from three domestic manufacturers for the SHINE project. To better characterize the radio frequency conditioning phenomena for validating the performance of power couplers, a room temperature test stand was designed, constructed, and commissioned for the SHINE 1.3 GHz power couplers. In addition, a horizontal test cryostat was built to test the 1.3 GHz superconducting cavities, fundamental power couplers, tuners, and other components as a set. The results of these tests indicate that the 1.3 GHz couplers are capable of handling up to 14 kW continuous waves. Herein, the main aspects of the radio frequency design and construction of the test stand, along with the test results of the high-power conditioning of the 1.3 GHz couplers, are described.

Full Text

Preamble

High RF Power Tests of the First 1.3 GHz Fundamental Power Coupler Prototypes for the SHINE Project

Zhen-Yu Ma, Shen-Jie Zhao, Xu-Ming Liu, Yue-Chao Yu, Hong-Ru Jiang, Xiang Zheng, Qiang Chang, Zi-Gang Zhang, Kai Xu, Yan Wang, Yu-Bin Zhao, Hong-Tao Hou

Shanghai Advanced Research Institute, Chinese Academy of Sciences, Shanghai
201204, China

Corresponding author: houhongtao@zjlab.org.cn

Abstract

The Shanghai High Repetition Rate XFEL and Extreme Light Facility (SHINE) project will utilize 600 fundamental power couplers (FPCs) operating at 1.3 GHz. These couplers are modified versions of the TTF-III design, adapted for continuous wave (CW) operation with input power up to approximately 7 kW. The first batch of 20 prototype coupler sets was fabricated by three domestic manufacturers for the SHINE project. To characterize radio frequency conditioning phenomena and validate coupler performance, a room-temperature test stand was designed, constructed, and commissioned specifically for the SHINE 1.3 GHz power couplers. Additionally, a horizontal test cryostat was built to evaluate the integrated performance of 1.3 GHz superconducting cavities, fundamental power couplers, tuners, and other components as a complete system. Test results demonstrate that the 1.3 GHz couplers can handle up to 14 kW in continuous wave operation. This paper describes the RF design and construction of the test stand, along with the high-power conditioning results for the 1.3 GHz couplers.

Keywords: Superconducting accelerating cryomodule, 1.3 GHz fundamental power coupler, RF conditioning, Test bench, Horizontal test cryostat

1 Introduction

The Shanghai High repetition rate XFEL and Extreme light facility (SHINE), currently under construction, represents China's first hard X-ray free-electron laser facility [?, ?, ?]. The SHINE facility will feature a superconducting linear accelerator with 8 GeV energy, three undulator lines, three beamlines, and the first ten experimental stations [?]. The linear accelerator comprises 75 superconducting cryomodules housing 600 1.3 GHz nine-cell TESLA-type superconducting cavities for electron beam acceleration, plus two third-harmonic superconducting cryomodules containing 16 3.9 GHz superconducting cavities for linearizing longitudinal phase space distortion [?, ?, ?, ?, ?].

Fundamental power couplers constitute one of the most critical components in superconducting cryomodules. The SHINE 1.3 GHz FPCs are modified and optimized from the TTF-III FPC design to meet project requirements [?, ?, ?]. Key modifications include shortening the cold part antenna by 8.5 mm to achieve a higher external quality factor Q_{ext} , increasing the copper plating thickness on the warm inner conductor to 150 μ m to mitigate overheating in CW mode, and machining the coaxial-to-waveguide transition directly from a single aluminum block—eliminating RF matching posts while enabling precision alignment. Additionally, the capacitor ring used for bias voltage was replaced

with a copper flex ring to provide superior RF sealing between the waveguide and coupler body. A stepper motor was also incorporated to remotely adjust coupling for various beam loadings and compensate for coupling changes due to inner conductor heating. The mechanical design of the SHINE 1.3 GHz FPC is illustrated in Fig. 1, with main technical parameters listed in Table 1.

The Q_{ext} of the superconducting cavity and power requirements can be calculated using Eqs. (1)-(3), which relate parameters including the coupling coefficient β , beam current I_b , cavity intrinsic quality factor Q_0 , cavity voltage V_c , cavity R/Q , frequency detuning δf , and resonant frequency f_0 [?]. For SHINE, the optimal Q_{ext} for 1.3 GHz superconducting cavities is 4.12×10^7 under the following conditions: average linac beam current of 0.3 mA, nominal accelerating gradient E_{acc} of 16.0 MV/m, cavity intrinsic quality factor Q_0 of 2.7×10^{10} , and frequency detuning δf of 10 Hz caused by peak microphonics effects [?, ?]. Considering a 15% waveguide transmission loss, the required input power from a solid-state amplifier (SSA) to maintain operating gradient is approximately 6.6 kW. Consequently, the 1.3 GHz FPC is designed to withstand 7 kW CW power with full reflection. The SHINE 1.3 GHz FPC features an adjustable mechanism with approximately 15 mm total antenna adjustment range, enabling Q_{ext} to span from 4.0×10^6 to 1.1×10^8 .

Prototype development began in mid-2018, and the first batch of 20 prototype sets has been fabricated by three domestic manufacturers and subjected to high RF power testing. The remainder of this paper is organized as follows: Section 2 briefly introduces surface preparation procedures for the 1.3 GHz FPCs. Section 3 presents the RF design of the test stand. Section 4 describes off-resonance high RF power conditioning and operation of the FPC prototypes in the cryomodule. Finally, conclusions are presented in Section 5.

2 FPC Preparation Procedures

Prior to assembly on the room-temperature test bench, FPCs must be cleaned to ultra-high vacuum standards to ensure faster and more efficient RF conditioning [?]. All FPC components were initially cleaned in an ultrasonic bath for 30 minutes, followed by rinsing with ultrapure water until the drain water resistivity exceeded $14 \text{ M}\Omega \cdot \text{cm}$ in a Class 10 cleanroom. Rinsed components were then dried using filtered high-purity nitrogen gas. Before final assembly, each component was again blown with filtered nitrogen while monitoring with a particle counter, which must register fewer than 10 particles >0.3 microns per cubic foot; otherwise, components returned to the ultrasonic bath [?]. Assembled FPCs underwent vacuum leak testing with helium leak detection sensitivity better than $1.0 \times 10^{-9} \text{ mbar} \cdot \text{L/s}$.

Baking has been found to reduce conditioning time by nearly a factor of two while providing better vacuum levels in FPCs prior to conditioning compared to non-baked units [?]. Assembled FPCs were baked under vacuum using a modified oven controlled via computer and programmable logic controller. The

standard baking procedure involved temperature ramping at 10 °C/h, holding at 150 °C for 72 hours to ensure complete water vapor removal, then cooling to room temperature at a controlled gradient of 10 °C/h. During baking, temperatures were monitored and gas species analyzed via residual gas analyzer. Vacuum and residual gas analysis results after baking are summarized in Table 2.

3 High RF Power Tests in the Room Temperature Test Bench

FPCs must undergo comprehensive high-RF-power conditioning at room temperature before installation with superconducting cavities in cryomodules. This process tests coupler robustness, conditions away residual absorbed gases, and “burns off” microscopic surface imperfections.

3.1 Composition of Room Temperature Test System for 1.3 GHz FPCs

The high RF power test system for 1.3 GHz FPCs comprises four major subsystems: (1) power source, (2) power transmission, (3) test bench, and (4) low-level control system [?, ?]. Figure 2 shows the system block diagram.

The power source system consists of a solid-state amplifier capable of 30 kW CW output. The transmission system includes various waveguides, circulators, water-cooled RF-absorbing loads, and short-circuit plungers. One RF-absorbing load connected to the circulator protects the power source by absorbing reflected power from the test bench, while another load absorbs all RF power reaching the terminal. A movable short-circuit plunger enables standing wave (SW) mode operation to ensure complete conditioning along all FPC positions. Incident and reflected RF power were measured using directional couplers. The test bench included a pair of back-to-back FPCs with a rectangular connection waveguide. Two ARC detectors monitored ceramic windows for arcing events, while six electron pick-up probes on the FPC outer conductors monitored secondary electron current and location. Ten thermocouples monitored FPC surface temperatures, and two IR sensors measured warm ceramic RF window temperatures.

The low-level control system monitored incident power, reflected power, temperature, vacuum, electron current, ARC events, and other signals, incorporating critical signals into an interlock system. When interlock signals exceed thresholds, the power source shuts down immediately to protect the FPCs [?]. Table 3 lists interlocking signal thresholds. For vacuum events exceeding 5.0×10^{-6} mbar, RF power cuts off immediately and resumes when vacuum pressure drops below 1.0×10^{-7} mbar. Real-time LabVIEW software provides the operator interface for adjusting RF mode parameters and controlling tests.

3.2 RF Design of 1.3 GHz FPC Test Bench

RF power transmission in the test bench proceeds as follows: the transverse electromagnetic (TEM) mode in the upstream FPC coaxial line couples to the rectangular connection waveguide via the antenna, exciting the transverse electric (TE₁₀) mode. Power then transmits through the rectangular waveguide to the downstream FPC antenna, continuing forward in the downstream FPC as TEM mode before reaching the terminal RF-absorbing load.

The RF design focuses on achieving good matching and minimizing power reflection. S-parameter optimization aims to minimize reflection coefficient and maximize transmission coefficient at the operating frequency. The rectangular connection waveguide was optimized based on a half-height WR650 waveguide (165.1 mm width \times 41.3 mm height), as shown in Fig. 3(a). Three structural parameters require optimization: antenna insertion depth h , distance between antenna and waveguide short-circuit surface d_1 , and distance between the two FPC antennas d_2 , as shown in Fig. 3(b).

Extensive simulations and calculations determined the optimal parameter combination: $h = 18.25$ mm, $d_1 = 63$ mm, and $d_2 = 175$ mm. With this configuration, the test bench with FPC antennas achieves optimal matching. Figure 4 shows S-parameter curves for the optimized test bench across 1.25-1.35 GHz, yielding a transmission coefficient $S_{21} \approx -0.0015$ dB and reflection coefficient $S_{11} \approx -54.28$ dB at 1.3 GHz.

Fabrication and installation errors can degrade transmission matching. A simple, practical solution involves adjusting antenna insertion depth to re-establish matching. Therefore, the influence of insertion depth h on S-parameters was further analyzed. The antenna insertion depth can be adjusted by ± 10 mm (i.e., h varying from 8.25 mm to 28.25 mm), causing the S_{11} peak frequency to shift from 1.3396 GHz to 1.2152 GHz, as shown in Fig. 5. Clearly, the S-parameter peak frequency can be tuned to 1.3 GHz by adjusting insertion depth to achieve optimal matching.

3.3 High RF Power Conditioning and Testing of the 1.3 GHz FPC Prototypes

S-parameters should be measured and matched before high RF power conditioning. The optimal measured values were $S_{11} = -42.84$ dB, $S_{22} = -55.35$ dB, $S_{21} = -0.0928$ dB, and $S_{12} = -0.0936$ dB, as shown in Fig. 6. From the S_{21} measurement, total power loss in the two FPCs and rectangular connection waveguide is 21 W for 1 kW input power.

To ensure stable FPC operation, units must transmit RF power significantly higher than 6.6 kW on the test bench. Typically, the RF conditioning target is twice the required power [?, ?]. Additionally, a special case was considered: if a cavity quenches during operation or trips for other reasons, all forward power reflects back, and the FPC experiences local peak power between minimum

value and four times the input level [?]. RF test specifications for SHINE 1.3 GHz FPC prototypes were established to evaluate manufacturing techniques and performance, as shown in Table 4.

FPCs were RF-conditioned in both traveling wave (TW) and SW modes. Conditioning began in TW pulse mode with 1 ms pulse length and 100 ms repetition period. Peak power increased from 1 kW to 28 kW in 0.5 kW steps, with power reduction if vacuum deterioration approached threshold. Maximum power was maintained for 30 minutes. Peak power then decreased to 1 kW, and the process repeated with sequentially increasing pulse widths of 2, 4, 8, 10, 15, and 20 ms. After pulse conditioning, CW conditioning commenced at 1 kW and increased to 14 kW in 0.5 kW steps, maintaining 14 kW CW for six hours. In SW mode, moving the short-circuit plunger through 170 mm ensured all FPC regions experienced maximum electric field. The SW mode conditioning procedure was similar to TW mode, maintaining 7 kW CW for twelve hours.

All 20 prototype sets were RF-conditioned and successfully passed high RF power tests on the room-temperature test bench. Figure 7 shows the test system. Results for one FPC pair are presented as representative examples. Figure 8(a) shows temperature distribution along the FPC as power increased from 5 kW to 14 kW in TW CW mode, while Fig. 8(b) shows distribution from 1 kW to 7 kW in SW CW mode. Temperature sensors at positions 2 and 5 monitored warm and cold RF window temperatures, respectively. In 14 kW TW mode or 7 kW SW mode, RF window temperatures remained below the 80 °C threshold, with no significant temperature rise in outer conductor bellows or the rectangular connection waveguide.

Figure 9(a) shows vacuum pressure in cold and warm parts from 5 kW to 14 kW in TW mode, while Fig. 9(b) shows vacuum variation during the six-hour 14 kW hold period. Figure 10(a) shows vacuum pressure from 1 kW to 7 kW in SW mode, and Fig. 10(b) shows variation during the 12-hour 7 kW hold period. Vacuum gradually improved during RF testing, with electron activity approximately 15 mV and ceramic RF window temperatures of 40-47 °C. Arcing events were rare during conditioning.

All prototypes were stored under vacuum until installation on superconducting cavities. After several weeks of vacuum storage, two prototypes were retested to verify RF conditioning memory. High RF power tests completed quickly and smoothly within 11 hours, confirming the storage method's effectiveness and reliability. Additionally, one prototype pair underwent extended testing at 4.5 kW SW power, producing equivalent heat load to SHINE's most stringent 0.3 mA beam current operation: 6.6 kW forward power with 1.6 kW reflected power (total 8.2 kW) at $Q_{ext} = 4.12 \times 10^7$. Power was maintained for 20 days without interlocking.

4 High RF Power Conditioning and Operation in Cryomodule

To minimize project risks, critical components and technical solutions are tested in the cryomodule under conditions approximating the final configuration [?, ?]. In this cryogenic test, eight 1.3 GHz superconducting cavities previously qualified in a vertical cryostat were fully assembled with all components (FPCs, magnetic shielding, feedthroughs, and tuners) in the cryomodule [?]. A primary goal was demonstrating that high Q_0 values from vertical tests could be preserved despite additional heating from FPCs, tuners, and potential external magnetic fields from auxiliary components. Other important verification studies included FPC thermal performance and power handling, HOM coupler and tuner component heating, tuner performance, microphonics sensitivity, and frequency control. This section focuses on FPC prototype test results.

4.1 Warm Off-Resonance RF Conditioning

The first SHINE 1.3 GHz cryomodule prototype was assembled and installed in a horizontal test tunnel in February 2021, as shown in Fig. 11. Eight 1.3 GHz FPC prototypes were installed. Warm off-resonance high RF power conditioning was performed in April 2021.

Initial conditioning of one FPC prototype verified test system functionality. The SSA master frequency was set to 1.3 GHz, approximately 1.7 MHz above the superconducting cavity resonant frequency to ensure off-resonance operation. Under 4.5 kW CW input, cavity vacuum changed from 1.2×10^{-8} mbar to 1.4×10^{-8} mbar, while FPC warm part vacuum changed from 1.8×10^{-8} mbar to 2.8×10^{-8} mbar (thresholds: cavity vacuum 1.0×10^{-7} mbar, FPC warm parts 5.0×10^{-7} mbar). Subsequent conditioning of five FPC sets at 4.5 kW input showed warm RF window temperatures of 40-50 °C, cavity vacuum changing from 1.3×10^{-8} mbar to 1.9×10^{-8} mbar, and FPC warm part vacuum changing from 1.6×10^{-8} mbar to 1.1×10^{-7} mbar. The remaining two FPC sets completed conditioning similarly. Figure 12 shows vacuum variation for all eight FPCs from 1 kW to 4.5 kW. Figure 13 shows temperature variation of warm RF windows and CF100 flanges, with maximum CF100 flange temperature increase approximately 25 K. No arc events or electron activities occurred during warm off-resonance conditioning.

4.2 Cold Off-Resonance RF Conditioning and Operation

The first 1.3 GHz cryomodule prototype was cooled to 2 K in July 2021, completed within several days. The loaded quality factor Q_L of cavities was measured and adjusted to the design value of 4.1×10^7 using two methods: (1) approximate direct measurement with coaxial waveguide and network analyzer, and (2) accurate power attenuation method. Table 5 lists Q_L measurements for eight cavities, with errors between methods not exceeding 10%. Due to a driving rod connection issue, FPC #8 could not be adjusted but this did not

affect subsequent high RF power conditioning.

Due to limited cryogenic system test time, FPCs were conditioned only to power levels sufficient for horizontal cavity tests. All FPCs were conditioned to 2.5 kW, with FPC #8 conditioned to 3.5 kW. Conditioning began with one FPC prototype at 2 K off-resonance, followed by three sets and then four sets conditioned together. Figure 14 shows vacuum variation for all eight FPCs from 0.5 kW to 2.5 kW. Figure 15 shows temperature variation of warm RF windows and CF100 flanges. At 2.5 kW input, maximum warm RF window temperature reached 45 °C. At 3.5 kW input to FPC #8, warm RF window temperature increased to 55 °C without cooling. At 2.5 kW input, cavity vacuum changed from 4.5×10^{-9} mbar to 4.3×10^{-9} mbar, while FPC warm part vacuum changed from 9.0×10^{-9} mbar to 1.0×10^{-8} mbar. Vacuum was minimally affected by high RF power conditioning at 2 K. Cold off-resonance conditioning for all eight prototypes completed in 19 hours without interlocking.

During the first horizontal tests of the integrated cryomodule prototype, establishing the 16 MV/m accelerating gradient required approximately 1.6 kW maximum input power. Vacuum, temperature, electron activities, and arcing events were monitored, and all eight FPC prototypes performed well.

4.3 Heat Flux Measurements at 5 K and 45 K Zones

FPC thermal intercepts comprising flexible copper braids provided effective cooling. One braid connected the FPC CF100 flange to the cryomodule's 45 K helium pipe, while another connected the 5 K intercept to the 5 K helium pipe. Cryogenic thermal paste ensured good thermal conduction between braids and clamping surfaces. Twenty-nine thermal sensors (Cernox and PT100) measured and monitored FPC temperatures at the 2 K, 5 K, and 45 K sections, plus the 5 K and 45 K copper braids. Heat flux for three FPC prototypes was calculated from temperature gradients on the copper braids.

Table 6 compares measured static heat loads between three SHINE 1.3 GHz FPC prototypes and the LCLS-II 1.3 GHz FPC prototype tested at Fermilab [?]. Reference values for 5 K and 45 K static heat loads were adopted from simulation results [?]. The 5 K static loads of SHINE prototypes are slightly lower than LCLS-II, while 45 K static loads are slightly higher. The 5 K static load of FPC #8 differed significantly from the other two prototypes, requiring verification of temperature sensor validity during future cryomodule disassembly.

Table 7 compares measured heat flux at 2.5 kW power level between three SHINE prototypes and the LCLS-II prototype. SHINE FPC prototypes demonstrate better heat load performance at both 5 K and 45 K zones. Note that LCLS-II's 45 K zones were connected to the cryostat's 80 K thermal shield, providing only a reference point.

Temperature rise saturation time for 45 K zone sensors was much longer than for 300 K and 5 K zones, determined by thermal conductivity of the FPC antenna,

ceramic window, massive CF100 stainless steel flange, and large-volume pure aluminum can attached to the CF100 flange. Over six hours of heating were required to approach equilibrium. In this test, temperature values were recorded after one hour; more accurate values will be obtained in future cryogenic tests.

6 Conclusion

The SHINE 1.3 GHz FPC was developed based on the XFEL TTF-III 1.3 GHz coupler with modifications and optimizations. The original TTF-III coupler was designed for 1 MW pulsed power but typically operated below 1.5 kW average power. Extrapolation of original test results suggested the TTF-III coupler could likely operate up to 5 kW SW, though without direct verification [?]. A room-temperature test stand with associated instrumentation, controls, and data acquisition systems was designed, assembled, and commissioned for RF testing of the 1.3 GHz FPCs. Twenty prototype sets were tested on the room-temperature RF test stand and transferred to cryomodule integration without encountering significant problems during conditioning. The first cryogenic horizontal test successfully validated the superconducting accelerating unit: 1.3 GHz superconducting cavities with helium tanks, FPCs, and tuners in the final cryomodule configuration achieved a nominal accelerating field of 16 MV/m with 1.6 kW input power.

For future CW accelerator projects where beam loading is small and microphonic detuning dominates the power budget, higher-power FPCs will be required. Based on current RF power test results, we believe 20 kW TW and 10 kW SW power levels are achievable for SHINE 1.3 GHz FPC prototypes, and this has been included in future research plans.

An automatic RF test bench has been installed and is currently being commissioned. The nominal RF conditioning rate of two couplers per week will be increased to four couplers within a few months.

Acknowledgements

We thank Dr. Yi-Yong Liu and Yawei Huang of Shanghai Advanced Research Institute, CAS, for discussions on static and heat flux measurement methods; Dr. Li-Xin Yin and Dong Wang of Shanghai Advanced Research Institute, CAS, for suggestions on FPC test plans; Dr. Denis Kostin of DESY for long-term assistance and guidance; and the SHINE cryomodule team for their dedicated work on the cryogenic horizontal test.

Funding

This work was supported by Shanghai Municipal Science and Technology Major Project (No. 2017SHZDZX02).

References

1. C. Feng, H.X. Deng, Review of fully coherent free-electron lasers. Nucl. Sci. Tech. 29, 160 (2018). <https://doi.org/10.1007/s41365-018-0490-1>
2. Z.T. Zhao, C. Feng, K.Q. Zhang, Two-stage EEHG for coherent hard X-ray generation based on a superconducting linac. Nucl. Sci. Tech. 28, 117 (2017). <https://doi.org/10.1007/s41365-017-0258-z>
3. Y.W. Gong, M. Zhang, W.J. Fan, et al. Beam performance of the SHINE dechirper. Nucl. Sci. Tech. 32(3), 29(2021). <https://doi.org/10.1007/s41365-021-00860-8>
4. Z.Y. Zhu, Z.T. Zhao, D. Wang et al., SCLF: an 8-GeV CW SCRF linac-based X-ray FEL facility in Shanghai, in Proceedings of the FEL2017, Santa Fe, NM, USA (2017). <https://doi.org/10.18429/JACoW-FEL2017-MOP055>
5. K. Liu, Q. Gu, J.Q. Zhang, et al. Digital low-level radio frequency system and cavity simulator for 1.3 GHz continuous-wave superconducting radio-frequency cavity. Nuclear Techniques, 44(05), 23-31 (2021). <https://doi.org/10.11889/j.0253-3219.2021.hjs.44.050203>
6. Y.X. Zhang, J. F. Chen, D. Wang, RF design optimization for the SHINE 3.9 GHz cavity. Nucl. Sci. Tech. 31(7), 73(2020). <https://doi.org/10.1007/s41365-020-00772-z>
7. X.Y. Pu, H.T. Hou, Y. Wang, et al. Frequency sensitivity of the passive third harmonic superconducting cavity for SSRF. Nucl. Sci. Tech. 31(3), 31(2020). <https://doi.org/10.1007/s41365-020-0732-x>
8. P.P. Gong, Y.B. Zhao, H.T. Hou, et al. Tuning control system of a third harmonic superconducting cavity in the Shanghai Synchrotron Radiation Facility. Nucl. Sci. Tech. 30(10), 157(2019). <https://doi.org/10.1007/s41365-019-0669-0>
9. Z.Y. Ma, J.F. Chen, Design optimization of 3.9 GHz fundamental power coupler for the SHINE project. Nucl. Tech. 132 (2021). <https://doi.org/10.1007/s41365-021-00959-y>
10. D. Kostin, E-XFEL Input Coupler Design and Simulations, Visit report of IRDA delegation at DESY (2016).
11. B. Dwersteg, D. Kostin, M. Lalayan, et al., Tesla RF Power Couplers in Proceedings of the 10th Workshop on RF Superconductivity (SRF2001), Tsukuba, Japan, pp.443-447.
12. T. Garvey, W.D. Möller, The RF power coupler development program at LAL-Orsay and DESY-Hamburg for TESLA and the European X-FEL, in Proceedings of the International Congress on Optics and Optoelectronics, Aug 2005, Warsaw, Poland.

13. J. Delayen, N. Meringa, On the Optimization of Q_{ext} Under Heavy Beam Loading and in the Presence of Microphonics, CEBAF-TN-96-022. May 1996.
14. H.T. Hou, Z.Y. Ma, S.J. Zhao, et al., Development of superconducting RF components for SHINE project, in Proceedings of 19th International Conference on RF Superconductivity, Dresden, Germany, 2019. <https://10.18429/JACoW-SRF2019-MOP049>
15. J.J. Guo, Q. Gu, M. Zhang, et al. Power losses caused by longitudinal HOMs in 1.3-GHz cryomodule of SHINE. Nucl. Sci. Tech. 30(7), 105(2019). <https://10.1007/s41365-019-0628-9>
16. H. Guler, W. Kaabi, A. Gallas, et al., XFEL COUPLERS RF CONDITIONING AT LAL, in Proceedings IPAC2016, Busan, Korea. <https://doi.org/10.18429/JACoW-IPAC2016-WEPMB006>
17. H. Jenhani, Preparation and conditioning of the TTF VUV-FEL power couplers, in Proceedings of 12th International Workshop on RF Superconductivity, Jul 2005, Ithaca, United States. Cornell University Press, ThP48, 2006. <http://hal.in2p3.fr/in2p3-00077431>
18. H. Jenhani, T. Garvey, P. Lepercq, et al., Developments in conditioning procedures for the TTF-III power couplers, in Proceedings of 10th European Particle Accelerator Conference (EPAC 06), Edinburgh, Scotland, 399-401.
19. L. Chen, S.H. Zhang, Y.M. Li, et al., Room-temperature test system for 162.5 MHz high power couplers. Nucl. Tech. 30(1), 7(2019). <http://10.1007/s41365-018-0531-9>
20. H. Jenhani, T. Garvey, A. Variola, RF conditioning studies of input power couplers for superconducting cavities operating in pulsed mode. Nucl. Instrum. Methods Phys. Res. A 595, 549 (2008). <http://10.1016/j.nima.2008.07.111>
21. H. Padamsee, J. Knobloch, and T. Hays, RF superconductivity for Accelerators. (Wiley-VCH, Berlin,2008), p:418.
22. F. Naito, K. Akai, N. Akasaka, et al., Input coupler for the KEKB normal conducting cavity, in Proceedings the PAC 1995. <http://10.1109/PAC.1995.505368>
23. M. Stirbet, I. E. Campisi, G. K. Davis, et al., Processing test stand for the fundamental power couplers of the spallation neutron source (SNS) superconducting cavities, in Proceedings of the PAC 2001. <http://10.1109/PAC.2001.986607>
24. M. Stirbet, RF conditioning: systems and procedures, report in high RF power couplers workshop (2002).

25. J. Knobloch, W. Anders, M. Martin, et al., CW Operation of the TTF-III Input Coupler, in Proceedings of the 2005 Particle Accelerator Conference. 3292-3294 (2005). <https://doi.org/10.1109/PAC.2005.1591445>.
26. D. Kostin, W.D. Moeller, Status and operating experience of the ttf coupler, in proceedings of the international linac conference (Linac2004), Luebeck, Germany, pp.156-158.
27. P. Sha, J.K. Hao, W.M. Pan, et al. Nitrogen doping/infusion of 650 MHz cavities for CEPC. Nucl. Sci. Tech. 32(5), 45 (2021). <https://10.1007/s41365-021-00881-3>
28. N. Solyak, I. Gonin, A. Gressellino, et al., Results of the cavity Integrated tests in Horizontal Test Stand at FNAL, LCLS-II technical note TN-15-43.

Figures

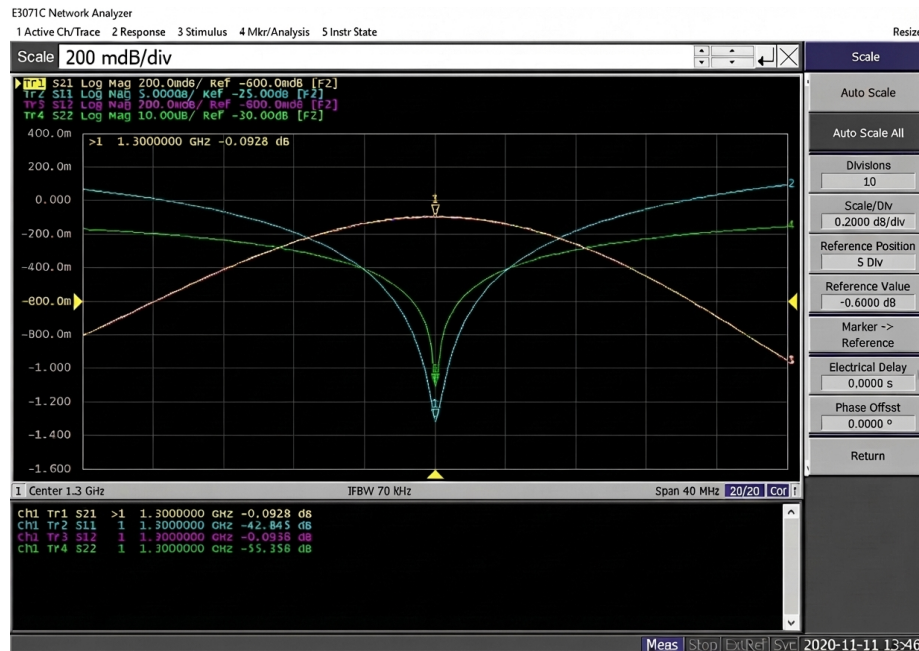


Figure 1: Figure 1

Source: ChinaXiv – Machine translation. Verify with original.

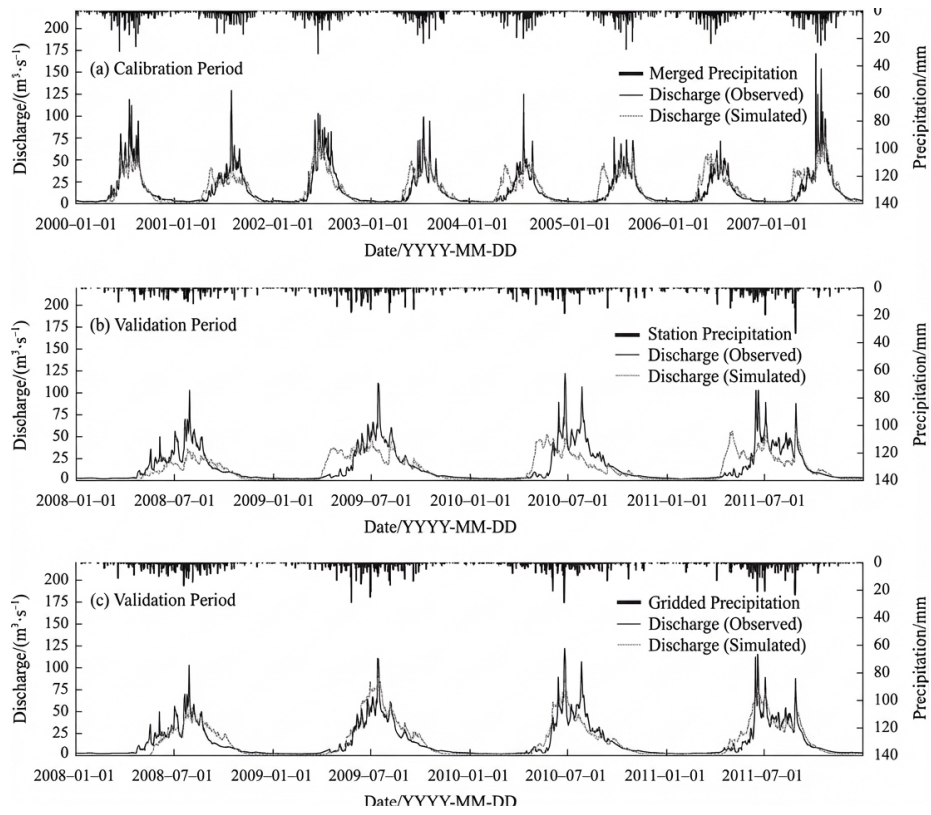


Figure 2: Figure 3

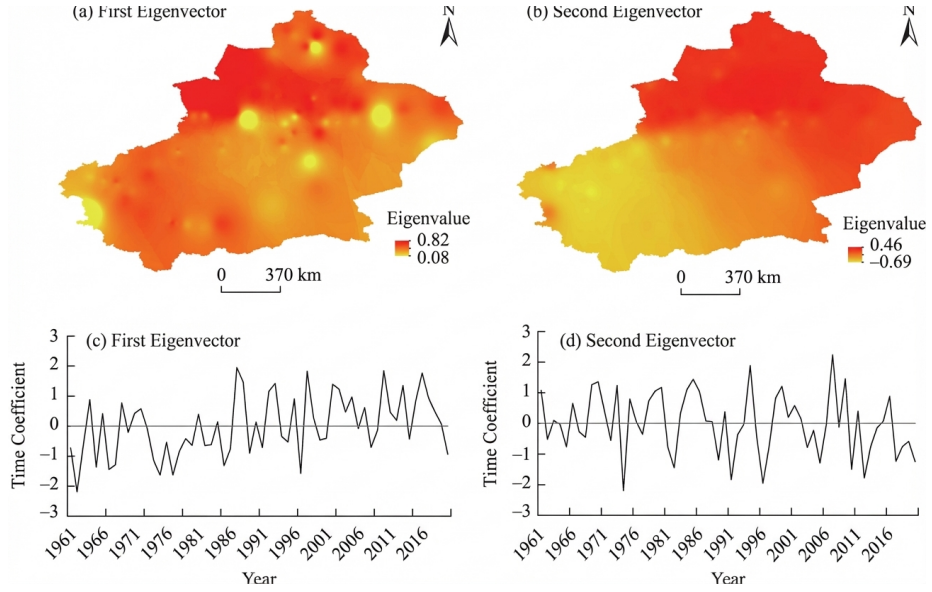


Figure 3: Figure 6

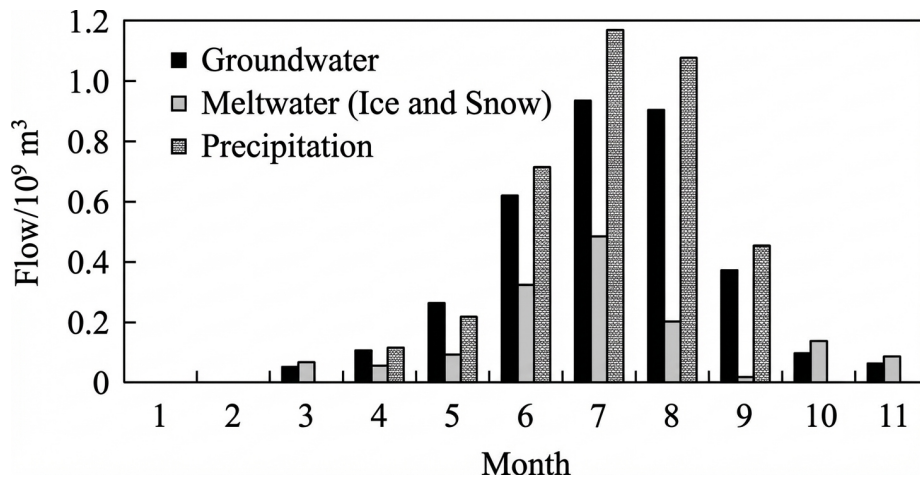


Figure 4: Figure 7

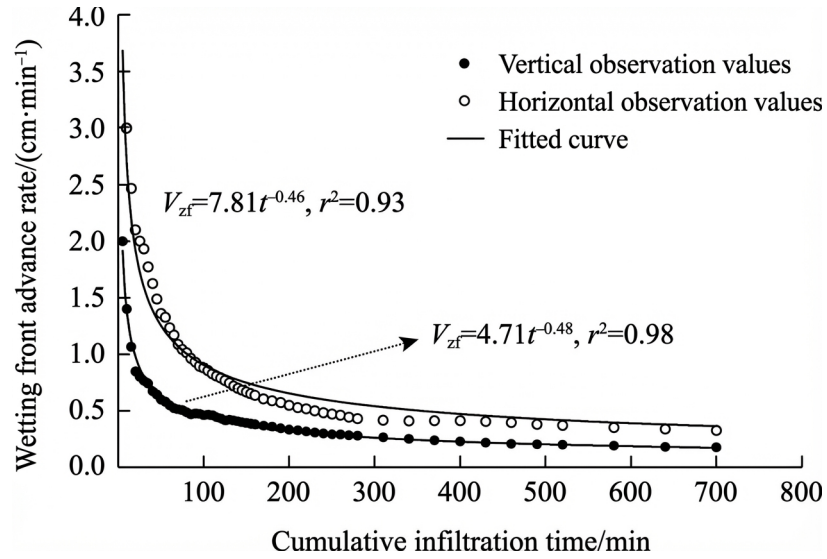


Figure 5: Figure 9

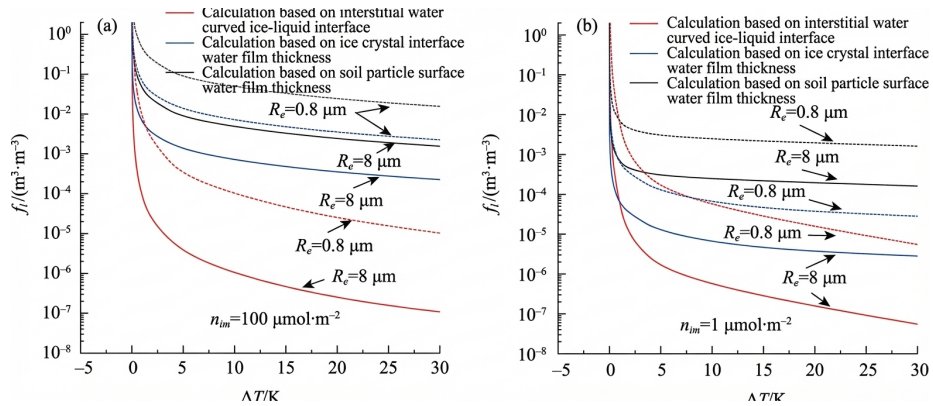


Figure 6: Figure 10

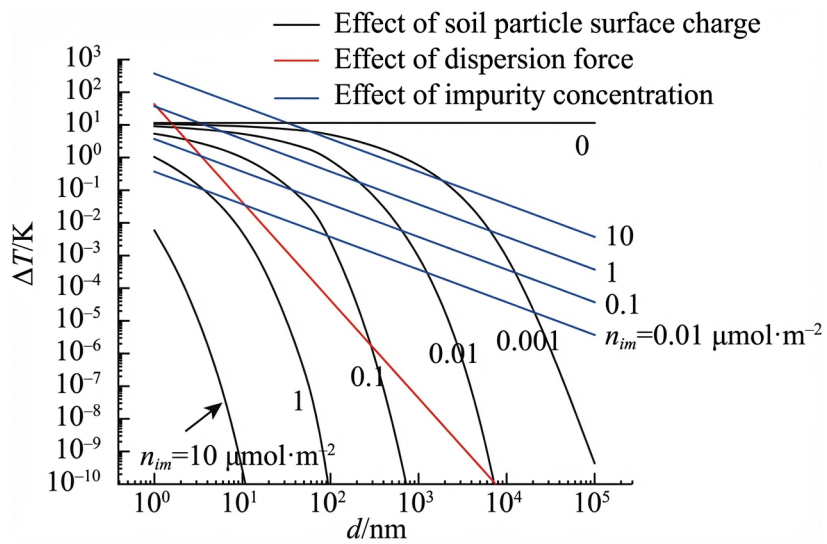


Figure 7: Figure 11